Spatially repeatable components from ultrafast ultrasound are associated with motor unit activity in human isometric contractions *

Journal of Neural Engineering

PAPER • OPEN ACCESS

Spatially repeatable components from ultrafast ultrasound are associated with motor unit activity in human isometric contractions*

To cite this article: Robin Rohlén *et al* 2023 *J. Neural Eng.* **20** 046016

Journal of Neural Engineering

PAPER

Spatially repeatable components from ultrafast ultrasound are associated with motor unit activity in human isometric contractions*

Robin Rohlén[1,2,6,**], **Marco Carbonaro**[3,4,6,**], **Giacinto L Cerone**[3,4], **Kristen M Meiburger**[4,5], **Alberto Botter**[3,4,7] and **Christer Grönlund**[2,7]

[1] Department of Biomedical Engineering, Lund University, Lund, Sweden
[2] Department of Radiation Sciences, Radiation Physics, Biomedical Engineering, Umeå University, Umeå, Sweden
[3] Department of Electronics and Telecommunication, Laboratory for Engineering of the Neuromuscular System (LISiN), Politecnico di Torino, Turin, Italy
[4] PoliToBIOMed Lab, Politecnico di Torino, Turin, Italy
[5] Biolab, Department of Electronics and Telecommunications, Politecnico di Torino, Turin, Italy
[6] These authors equally contributed to the work.
[7] These authors share senior authorship.

* A B holds a patent on electrode technology for joint EMG and ultrasound acquisitions (WO2014009868A2). Other authors declare no competing interests.

**Authors to whom any correspondence should be addressed.

E-mail: robin.rohlen@bme.lth.se and marco.carbonaro@polito.it

Keywords: motor unit, ultrafast ultrasound, electromyography, decomposition, territory

Supplementary material for this article is available online

OPEN ACCESS

RECEIVED
19 April 2023

REVISED
26 June 2023

ACCEPTED FOR PUBLICATION
12 July 2023

PUBLISHED
26 July 2023

Abstract

Objective. Ultrafast ultrasound (UUS) imaging has been used to detect intramuscular mechanical dynamics associated with single motor units (MUs). Detecting MUs from ultrasound sequences requires decomposing a velocity field into components, each consisting of an image and a signal. These components can be associated with putative MU activity or spurious movements (noise). The differentiation between putative MUs and noise has been accomplished by comparing the signals with MU firings obtained from needle electromyography (EMG). Here, we examined whether the repeatability of the images over brief time intervals can serve as a criterion for distinguishing putative MUs from noise in low-force isometric contractions. *Approach.* UUS images and high-density surface EMG (HDsEMG) were recorded simultaneously from 99 MUs in the biceps brachii of five healthy subjects. The MUs identified through HDsEMG decomposition were used as a reference to assess the outcomes of the ultrasound-based components. For each contraction, velocity sequences from the same eight-second ultrasound recording were separated into consecutive two-second epochs and decomposed. To evaluate the repeatability of components' images across epochs, we calculated the Jaccard similarity coefficient (JSC). JSC compares the similarity between two images providing values between 0 and 1. Finally, the association between the components and the MUs from HDsEMG was assessed. *Main results.* All the MU-matched components had JSC > 0.38, indicating they were repeatable and accounted for about one-third of the HDsEMG-detected MUs (1.8 ± 1.6 matches over 4.9 ± 1.8 MUs). The repeatable components (JSC > 0.38) represented 14% of the total components (6.5 ± 3.3 components). These findings align with our hypothesis that intra-sequence repeatability can differentiate putative MUs from noise and can be used for data reduction. *Significance.* This study provides the foundation for developing stand-alone methods to identify MU in UUS sequences and towards real-time imaging of MUs. These methods are relevant for studying muscle neuromechanics and designing novel neural interfaces.

1. Introduction

Recently, neuromuscular imaging based on ultrafast ultrasound (UUS) has evolved considerably, opening new fronts in studying muscle contraction at the single motor unit (MU) level [1–9]. High-resolution imaging of active muscle tissue can provide spatiotemporal mechanics of individual MU fibres, i.e. a 2D image with the location of the MU territory and the time course of its displacement velocity. Hence, the technique provides complementary information, such as *mechanical* information with access to *deep* muscles, to the standard electrophysiological techniques for assessing single MU *electrical* properties, i.e. invasive needle electromyography (nEMG) [10–12] and non-invasive surface EMG (sEMG) [13, 14]. The added information on spatial and temporal mechanics can foster basic studies on muscle neuromechanics and force generation mechanisms [15], along with providing biomarkers for myopathic disorders [16–18], and innovative neural interfaces relevant, e.g. in rehabilitation and prosthetic control [19–21].

The methodology of identifying single MU activity in UUS recordings during isometric *voluntary* contractions was recently proposed based on a two-step approach [3]. First, the subtle intramuscular displacement velocities were estimated [22], and then these displacement velocities were decomposed into multiple components. Each component comprises a *spatial* map (2D image with the location of the component, related to MU territory) and a *temporal* signal (time course of its displacement velocity, related to MU spike train). To separate spurious components (noise) from those associated with single MU activation, a procedure based on *temporal* signal characteristics was adopted and later validated against single MU identification based on needle EMG [4]. It was found that a large proportion of the components' temporal twitch-by-twitch signals could not be matched with MU firings [4, 6]. Two factors may contribute to this relatively low agreement between the two measures. The first is the heterogenic composition of linear and non-linear elastic tissue constituents, causing a non-linear combination of MU twitches. The second one concerns MU firing variability. Indeed, although the MU pool should be stable during these contractions, the firing rate of MUs varies, which has been shown to influence the temporal twitch parameters, i.e. alter the temporal signal (sequence of twitches) [15].

In contrast to the temporal firing characteristics, the location of MU fibres within the muscle cross-section should represent an invariant feature during constant force and isometric contractions. It follows that components with a stable spatial map throughout the contraction are more likely to be associated with actual MU activations. Hence, we hypothesise that the spatial repeatability of a component across short epochs (intra-sequence repeatability) is a feature associated with MU activity and may be used as a criterion for data reduction of the initial decomposed components.

In this study, we aimed to identify intra-sequence spatially repeatable components and examine whether repeatability can be used to separate MUs from noise in stable low-force isometric contractions. For this purpose, we decomposed displacement velocity images in consecutive two-second epochs from eight-second UUS recordings of the biceps brachii muscle. We quantified the repeatability of the components' spatial map across epochs and examined whether the repeatable components were associated with actual MU activity. To this end, we used a set of reference MUs identified with an independent and validated decomposition method (HDsEMG decomposition [23]), applied to experimental signals detected simultaneously with the ultrasound images. Finally, we determined whether the analysis based on two-second intervals (required to assess the repeatability) affects the number of MU-matched components compared with the decomposition of the recordings' full length (eight seconds).

2. Methods

2.1. Experimental protocol

A total of 99 MUs was extracted from five subjects (31 $\pm$ 6 years, three males, and two females) who performed three low-level isometric constant-force elbow flexions to activate the biceps brachii muscle (from 2% to 10% of the maximum voluntary contraction). Since we focus on the MU and not the subject per se, the number of MUs can be seen as the sample size. It is important to include both male and female participants, as it has previously been found that surface EMG has limitations in identifying MUs due to the differences in volume conduction [24]. In contrast, UUS has a deeper penetration and therefore does not have this issue. The details of the experimental protocol are reported in Carbonaro *et al* [6]. Briefly, for each contraction, eight-second-long UUS recordings (Verasonics Vantage 128, Verasonics Inc., Kirkland, WA) were recorded simultaneously [25] with HDsEMG (MEACS, LISiN, Politecnico di Torino, Turin, Italy [26]). A grid of 64 surface-EMG electrodes transparent to ultrasounds (8 $\times$ 8, 10 mm inter-electrode distance [27]) was placed on the muscle belly with the ultrasound transducer (L11-5v, 7.81 MHz centre frequency, 31.25 MHz sampling rate, and 2500 Hz frame rate) positioned between the fourth and the fifth row of electrodes; i.e. transversally with respect to the muscle fibres' direction (figure 1(A)). The study was conducted following the Declaration of Helsinki and approved by the Regional Ethics Committee. Informed consent was obtained from all subjects.

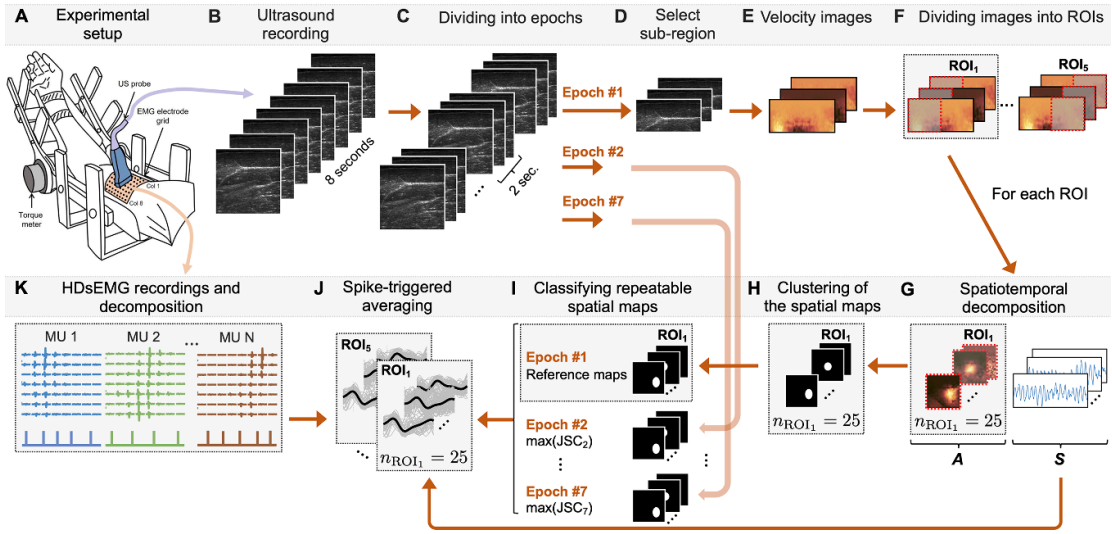

Figure 1. Illustration of the ultrasound data processing and identification of repeatable spatial maps. (A) Experimental setup with simultaneous ultrafast ultrasound (UUS) and high-density surface electromyography (HDsEMG) recordings. Reproduced from [6]. CC BY 4.0. (B) Eight-second recordings using UUS (40 × 40 mm, 2500 Hz) plane wave imaging. (C) The recordings were divided into seven partially overlapping epochs of two seconds each. (D) A sub-region was selected within the HDsEMG detection volume (20 × 40 mm). (E) Tissue velocity images were estimated. (F) The velocity images were divided into five region-of-interests (ROIs), i.e. 20 × 20 mm each. (G) Each ROI was decomposed into 25 components, i.e. 25 temporal signals ('S') and 25 spatial maps ('A'). (H) The spatial maps were clustered and processed to generate a binary map, with zeros being the background and ones being the largest intensity of the territory. (I) The binary maps were used for calculating the Jaccard similarity coefficient (JSC) for each component in the epoch (second to the seventh) with the first epoch as a reference. The maximal JSC was retained for each epoch, and then the mean JSC (based on the maximal JSC for all epochs) was calculated. (J) Then, spike-triggered averaging of the components' temporal signal was performed using the motor unit (MU) spike trains instants from the (K). HDsEMG decomposition.

2.2. UUS and HDsEMG data processing

The radio frequency UUS data comprised 20 000 frames (2176 × 128 pixels, i.e. approximately 53 × 40 mm). After traditional delay-and-sum beamforming, each eight-second dataset was processed in two-second epochs [3, 4] with one-second overlapping ([0:2] s, [1:3] s, …, [5:7] s, [6:8] s) resulting in seven sub-datasets of two seconds (figure 1(C)). Each pixel in each sub-dataset was filtered over time with a 1D median filter with the order equal to 10 ms [3, 4]. The image was cropped to 20 × 40 mm (850 × 128 pixels) [6, 7] (figure 1(D)). For each epoch, displacement velocity images were calculated using 2D autocorrelation velocity tracking [22, 28] with 1 mm in-depth and a sliding window of 10 ms (figure 1(E)). The temporal evolution of each pixel in the velocity images was high pass filtered at 3 Hz using 3rd order Butterworth filter (zero-phase) to attenuate slow movements not associated with muscle contraction [3]. Finally, the velocity images were down-sampled to 63 × 128 pixels, corresponding to approximately 0.3 × 0.3 mm per pixel.

HDsEMG signals were bandpass filtered (20–400 Hz) and decomposed into individual MU spike trains [23] (figure 1(K)). The spike trains were edited [29] and resampled at the ultrasound frame rate. MU action potential (MUAP) amplitude distributions and their centroids were calculated using the longitudinal single differential MUAP decomposed from HDsEMG [30]. Considering that the mediolateral surface covered by the HDsEMG grid is larger than that of the ultrasound transducer (figure 1(A)), all the centroids with the mediolateral coordinate outside the ultrasound field of view were truncated to the position of the first or last element of the probe (i.e. element 1 or 128).

2.3. Spatiotemporal decomposition of displacement velocity images

As described in previous papers, the displacement velocity images were processed over five partially overlapping region of interest (ROI) of 20 × 20 mm (5 mm increments) [4, 6, 8] (figure 1(F)). We used spatiotemporal independent component analysis (stICA) [31] with $\alpha = 1.0$ [8] to obtain 25 spatial components (*spatial maps*) and corresponding temporal components (*temporal signals*) per ROI [4, 8] (figure 1(G)). Hence, we obtained 125 spatiotemporal *ultrasound components* for each recording.

To generate a binary map suitable for comparison across epochs, we used the *k*-means algorithm (figure 1(H)). We used five clusters based on Euclidean distance because it provided an automatic robust way (empirically) of thresholding each decomposed spatial component regardless of the distribution of pixel values (see discussion and figure S2 in the supplementary materials). The cluster with the highest intensity values was assumed to be the localised spatial region (territory) of interest (figure S2 in the supplementary materials). Given this cluster, a binary map was generated. Objects with less than 25

connected pixels ($\sim$1.5 $\times$ 1.5 mm^2) were removed to remove noisy pixels at other regions in the image.

2.4. Repeatability analysis: selecting similar spatial maps across epochs

A Jaccard similarity coefficient (JSC) criterion based on the binary maps was used to select a set of similar spatial maps across different time epochs. The JSC is a metric used for comparing the similarity between two binary images, where pixel values can be equal to one, which highlights the object, or zero, which represents the background. Here, the 2D MU territory is the object consisting of the ones in the image, whereas the pixels outside the territory are assumed to be zeros. The JSC is defined as the *ratio* between the *area of overlap of ones* between the two images and the *area of ones from both images combined.* JSC values range from 0 (no overlap between the objects, which means the two images are not similar) to 100% or 1 (the two objects are perfectly overlapped and coincide).

Specifically, the 25 spatial maps of the *first two-second epoch* for each ROI were regarded as *reference* maps (figure 1(I)). JSCs were calculated between each *reference* map and the 25 maps obtained from each of the remaining six epochs. For each epoch, the map with the highest JSC was retained. This procedure provided, for each *reference* map, a selection of six spatial maps maximally similar to it. The *mean spatial map* and *mean JSC* (indicating the level of repeatability of a component) were then computed using the selected maps. In total, 25 mean spatial maps were identified for each of the five ROIs (125 mean spatial maps, including all five ROIs).

2.5. Association of selected similar components with MUs from HDsEMG

We studied the association between the ultrasound components selected in the previous paragraph and the characteristics of individual MUs identified through HDsEMG decomposition. To this end, we considered the *temporal* signal corresponding to the selected spatial maps and the firing pattern of the MUs identified from HDsEMG.

The *temporal* signals of each set of selected components were spike-triggered averaged (figure 1(J)) using the spike train of individual MUs identified from HDsEMG (figure 1(K)). This procedure was applied to all the combinations of selected ultrasound components and HDsEMG MUs, leading to a large set of *putative twitches* (figure 1(J)). Only those whose peak-to-peak amplitude exceeded a noise threshold were retained among these putative twitches. Among this subset, the pair (ultrasound component—HDsEMG MU) leading to the highest twitch amplitude was called the *MU-matched* component.

The noise threshold was calculated based on a three-step approach. First, we generated 125 temporal components of coloured Gaussian-distributed noise (5–30 Hz bandwidth of white noise) and 100 random spike trains (mean firing rates between 8 and 20 Hz and standard deviation of 15% of the mean inter-pulse interval [32]). Second, we calculated the spike-triggered averaging using the generated components and spike trains and calculated the peak-to-peak amplitudes of these 'average noise-twitch' (in the supplementary materials, figure S3 shows the distribution of all the amplitudes calculated with this procedure). Note that each triggered window was standardised with mean zero and standard deviation equal to one (z-score), making the spike-triggered averaging amplitude independent. Third, the threshold value was computed as the mean *plus* three standard deviations of the peak-to-peak amplitudes of all random components and spike trains (figure S3). Hence, the noise threshold is set as an 'outlier' of the peak-to-peak noise amplitude distribution.

2.6. Number of matched components with MUs from HDsEMG: intra and full sequence approach

We intended to assess whether the analysis on two-second intervals, required to assess the repeatability, affected the number of MU-matched components. Therefore, we compared the number of MU-matched components found with the *intra-sequence* repeatability approach with the components decomposed from the stICA applied over the *full sequence recording* [4]. In both approaches, the matching with HDsEMG MUs was performed using the same method described in the previous paragraph.

2.7. Statistical analysis

We calculated descriptive statistics associated with the components (epochs and full sequence) and the MUs decomposed from HDsEMG. The quality of identified MUs from HDsEMG was quantified using the pulse-to-noise ratio (PNR) [33]. Based on the matched components with MU, we calculated the area, equivalent diameter (square root of 4 $\times$ Area/π as in [3]), and depth of the centroid of the component below the skin. In addition, the distance between the mediolateral centroids of the spatial map (based on the binary map) and MUAP spatial distribution (based on the spike-triggered average on the HDsEMG signals using the MU spike trains [30]) for each matched component and MU was calculated.

We tested the pairwise difference between the number of MU-matched components between the intra-sequence repeatability and the full sequence approach using a two-sided Wilcoxon signed rank test. In addition, we tested the difference in median

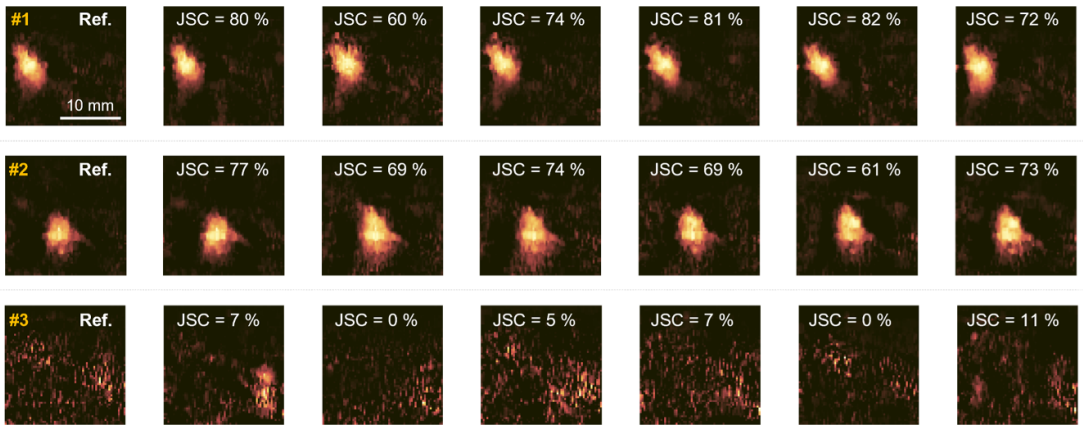

Figure 2. Examples of repeatable spatial maps from two repeatable components (#1 to #2) and one non-repeatable component (#3) of the same recording and region-of-interest (ROI) based on the Jaccard similarity coefficient (JSC). The first two-second epoch is the reference (defined as reference).

JSC and normalised peak-to-peak amplitude, respectively, between the MU- and non-MU-matched components using the Mann–Whitney *U* test. The significance level was set to 0.05.

3. Results

Out of 20 recordings, 99 MUs (4.9 ± 1.8 MUs per recording) were identified by decomposing HDsEMG signals having a PNR of 27.4 ± 3.1 dB. The MUs had stable spike trains over the eight-second recordings with firing rates of 12.3 ± 2.1 Hz.

We observed various degrees of intra-sequence repeatability across the 125 ultrasound components per recording, as shown by the large variability of JSC values (figure S1 in supplementary material). Figure 2 depicts two examples of repeatable components (high mean JSC) and one non-repeatable component (low mean JSC) from one ROI of a representative subject recording.

3.1. Association of selected similar components with MUs from HDsEMG

The scatterplot of figure 3 shows the relationship between JSC values and the amplitude of the (spike-triggered averaged) *putative twitches* from all subjects and trials. Each data point in figure 3 represents an ultrasound component and an HDsEMG MU that provided the *putative twitch* with the highest amplitude. Those below the noise thresholds (grey dots in figure 3) were discarded among these data points. In some instances, the above threshold *putative twitches* (coloured dots in figure 3) was obtained by combining the same MU and different ultrasound components. In these cases, the combination leading to the highest *putative twitch* was retained (*MU-matched* components, red circles in figure 3). The *MU-matched* components had a higher JSC than the *non-MU-matched* (grey dots) components (0.61 ± 0.12 vs 0.26 ± 0.26; $p < 0.001$) (figure 3). Noteworthy, the *MU-matched* components had a mean JSC always greater than 0.38, suggesting good repeatability (figure 2). In addition, defining the components as *repeatable* using this empirical threshold of 0.38, each recording had 6.5 ± 3.3 repeatable components.

Figure 4 shows three representative examples illustrating the spatial agreement between MUAP distributions and spatial maps of the *MU-matched* components together with the corresponding velocity twitches obtained with spike trigger averaging over all the MU firings of all epochs.

MU-matched components were spatially (mediolaterally) adjacent to the MUAP distribution (table 1), as demonstrated by the mediolateral distance between the centroid of the MUAP distributions and the centroid of the spatial maps (5.35 ± 5.17 mm, $N = 35$ MU). The centroids of the mean spatial maps were distributed across the whole field of view with depths between 2.90 mm and 14.01 mm (table 1). In addition, the *MU-matched* components had a diameter of 4.03 ± 1.28 mm, similar to previously reported findings of MU territory size using scanning-EMG [34].

3.2. Number of matched components with MUs from HDsEMG: intra and full sequence approach

The intra-sequence analysis led to 35 *MU-matched* components, i.e. 35.4% of the MUs identified by HDsEMG (table S1, supplementary material). By decomposing the full eight-second UUS, we found 36 matches, i.e. 36.4% of the MUs identified by HDsEMG. We found no difference in the number of matched MUs across all recordings concerning the two approaches ($p = 0.9844$).

4. Discussion

This study investigated whether the spatial repeatability of components extracted from UUS sequences can be used as a criterion to separate muscle tissue

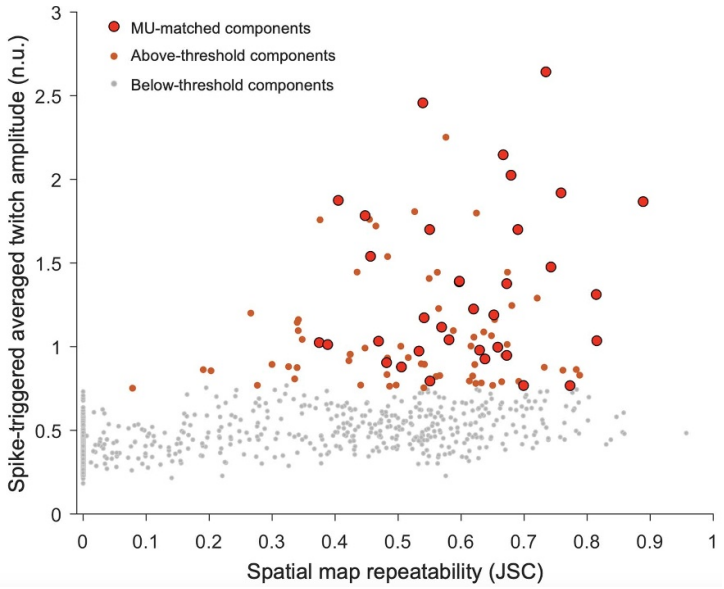

Figure 3. Relationship between Jaccard similarity coefficient (JSC) and putative twitches with the highest spike-triggered averaged twitch amplitude. Grey dots are the putative twitches below the noise threshold that were discarded. The red circles correspond to the 35 MU-matched components. All the MU-matched components have JSC over 0.38 (i.e. repeatable). Orange dots refer to multiple components associated with the same MU (e.g. twisting/split territory, duplicate components, etc, see figure 5).

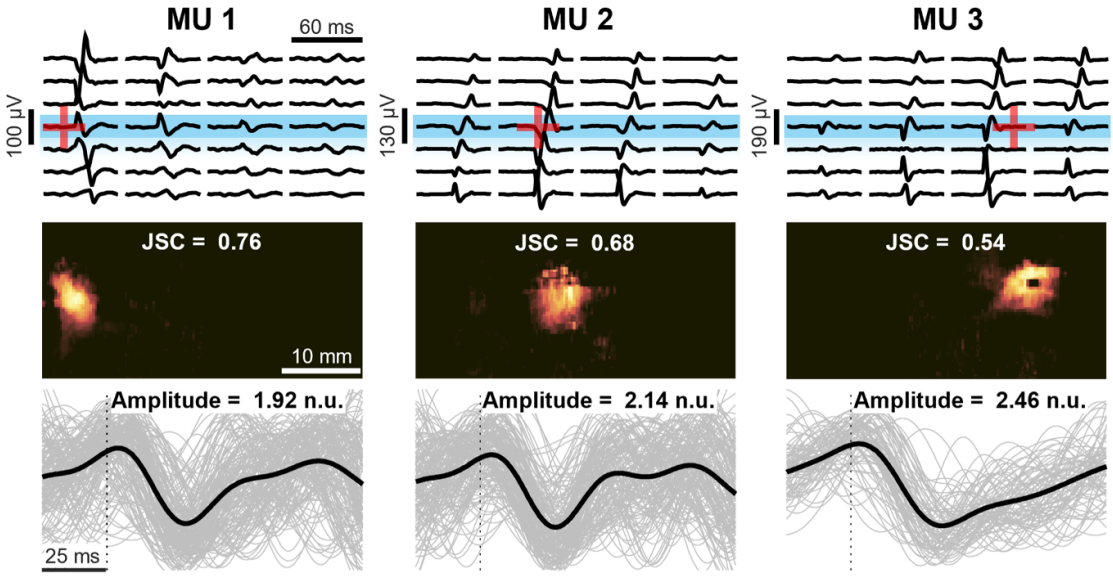

Figure 4. Three representative matches between repeatable components and the motor units (MUs). The upper panels show the MU action potentials and the centroid of the EMG distribution (red '+'). In this representation, only the four columns of the EMG grid superimposed on the ultrasound probe (blue rectangle) are shown. The middle panels show the mean spatial map of the repeatable component and the corresponding mean JSC. Finally, lower panels depict the spike-triggered averaged velocity twitch (black line) based on the triggered signals from all seven epochs (grey lines) and the corresponding peak-to-peak amplitude. The vertical dotted lines corresponded to the firing instants of the MUs identified from HDsEMG decomposition and used for the triggering.

displacements associated with single MU activation from noise during stable low-force isometric contractions. First, we decomposed displacement velocity sequences from consecutive two-second epochs of eight-second UUS recordings. Then, we quantified the repeatability of the components' spatial map across epochs and examined whether there was an association between the repeatability level and the degree of matching with reference MUs identified through HDsEMG decomposition. Finally, we investigated whether this intra-sequence approach using short epochs affects the number of matched MUs by comparing it with the decomposition of the recordings' full length (eight seconds). We obtained three main findings: (1) all the MU-matched components had a JSC larger than 0.38 and accounted for about one-third of the HDsEMG-detected MU, (2) the components with JSC $>$ 0.38 represented

Table 1. Descriptive statistics about the motor unit-matched repeatable components.

MU-matched repeatable components	$N = 35$
Jaccard similarity coefficient, JSC	0.61 ± 0.13 (0.38; 0.89)
Amplitude (n.u)	1.35 ± 0.49 (0.76; 2.64)
Centroid-to-centroid (EMG-UUS) (mm)	5.35 ± 5.17 (0.01; 15.83)
Depth (mm)	9.47 ± 2.40 (2.90; 14.01)
Diameter (mm)	4.03 ± 1.28 (1.45; 7.25)
Area (mm^2)	14.06 ± 8.71 (1.66; 41.30)

Mean ± SD (min; max), MU = motor unit, EMG = electromyography, UUS = ultrafast ultrasound, n.u. = normalised units.

approximately 14% of the 125 initial components from each recording, and (3) the number of MU-component matches did not differ between the intra- and full-sequence approaches. These findings imply that spatially repeatable components from UUS are associated with MU activity in human isometric contractions, where the UUS decomposition method can identify possible MU activity in recordings as short as two seconds.

About 14% of the spatiotemporal components identified applying stICA to UUS sequences were matched with MUs decomposed independently from HDsEMG. A common characteristic of all the *MU-matched* components was the high JSC (figure 3) of their spatial maps. This evidence suggests that spatial repeatability across a short epoch is a relevant feature useful to identify putative MUs and implement data reduction methods on the initial set of ultrasound components. This result confirms the initial hypothesis, i.e. since the location of the MU fibres is an invariant feature of the MU during stable isometric contractions, *repeatable* spatial maps are more likely to be associated with actual MUs. Whether this hypothesis applies to conditions other than isometric or constant force contractions likely depends on how MU territory is represented in the ultrasound scanning plane and how this representation changes during a contraction. For instance, muscle shape changes occurring during dynamic contractions may lead to a shift or a shape change of the area where MU fibres' activation induces movement within the muscle cross-section, i.e. within the ultrasound scanning plane. This would clearly undermine the assumption of MU territory spatial invariance, which is the basis for our hypothesis. Although to a lesser extent, similar variations in MU territory representation can also occur during isometric contractions, for instance, during force-varying contractions, fatiguing contractions or any condition inducing a progressive MU recruitment or de-recruitment. Further studies are required to quantify the effects of these factors on UUS decomposition.

About one-third of MUs decomposed from HDsEMG matched with repeatable ultrasound components. This is similar to the number of successful identifications found in previous studies. It has been previously associated with differences in detection volume and characteristics of two detection systems (EMG and ultrasound) [4, 6, 35]. In addition to the characteristics of the two measuring techniques, it is worth noting that the measured system is expected to be non-linear due to the heterogenic composition of linear and non-linear elastic constituents. Already at 5%–10% MVC, many MUs are active and may suppress or distort the triggered twitch amplitude. Another aspect to consider is that, in this study, we found more repeatable ultrasound components for each recording (6.5 ± 3.3) than HDsEMG MUs (4.9 ± 1.8). Although ultrasound provides a larger field of view and higher spatial resolution than HDsEMG, it remains unclear whether these unmatched repeatable components are MUs and whether they identify different MUs in the whole active MU population. In the present study, the number of successful identifications may have been biased by one subject for which our matching criteria led to no matched MUs. This case was most likely due to the poor quality of the displacement velocity images. The exclusion of this subject would have increased the percentage of MU-matches from 35.4% to 42.7% for the intra-sequence repeatability approach and from 36.4% to 43.9% for the original decomposition over the full sequence (table S1, supplementary material).

Decomposing displacement velocity images into components using stICA over partially overlapping windows likely resulted in component duplicates. Figure 5(a) shows two examples of duplicates in which three different components decomposed in three consecutive ROIs showed an amplitude of the twitches (related to the same MU firings) over the noise threshold. In this case, the component providing the highest twitch amplitude was selected and regarded as the MU-matched component. Moreover, it is worth noting that the stICA approach we used assumes spatial independence to decompose the dataset [31, 36]. For this reason, it may split MU territories into separate components if the MU activation results in complex movements, e.g. due to the interaction between active and passive tissue [37, 38] or tissue rotation due to so-called MU twisting [1, 7]. All these examples of duplicate components are now separated and contribute to the above-threshold components in figure 3 (small orange points). In future studies, components belonging to the same MU may be merged considering the spatial overlay or a correlation approach based on, e.g. the temporal signals.

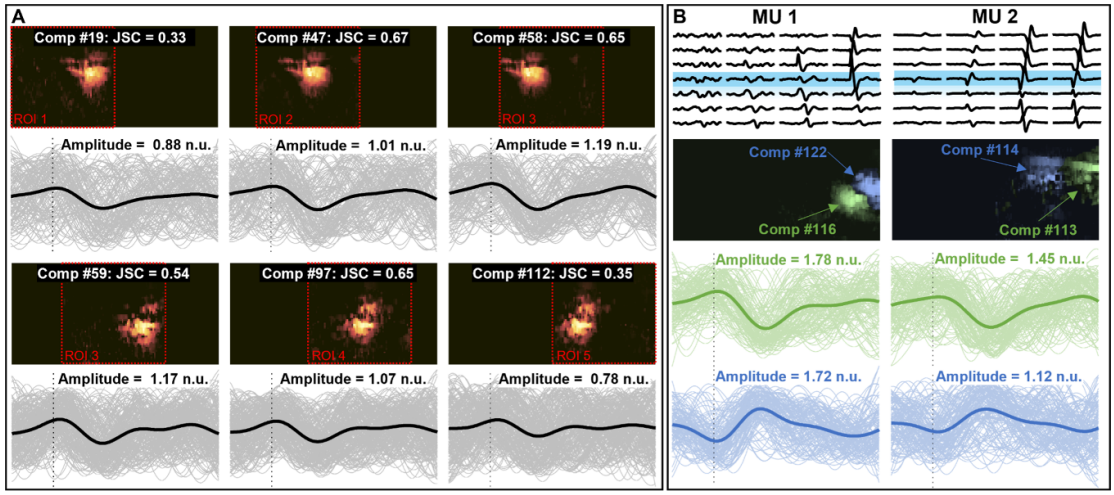

Figure 5. Examples of multiple components associated with the same MU. (A) Two examples of three different components (belonging to different ROIs) with a similar spatial map (active region) matched with the same MUs. In this case, the three components were merged into the same repeatable component. (B) Two examples of possible twisting MUs. The MUs were matched with two components showing active regions close to each other and the average twitches showing opposite profiles. Green twitches are negative (movements towards the probe/skin), and blue twitches, on the contrary, are positive (movements away from the probe/skin).

This study also found that MUs have a twisting property (figure 5(B)), as observed in previous research [1, 7]. Here, two components (matched with the same MU) are spatially separated in two regions of activation (blue and green spots in figure 5(B)) close to each other with inverted twitch shapes (blue and green twitches in figure 5(B)). The shape of the twitch is related to the direction of the movement with the green twitches are negative (i.e. towards the probe/up), while the blue ones are positive (i.e. away from the probe/down). Interestingly, the MU twisting may deeper explain observations done with several MMG techniques reflecting the deflections of muscle surface for isolated MUs in rats [39] and human muscles [40]. To further understand the deformation of the muscle fibres during a contraction, we should consider 3D imaging as we will likely have out-of-plane motion.

Although finding repeatable components requires eight seconds with the intra-sequence approach herein proposed, the results of this study confirm previous studies that the UUS decomposition method can identify possible MU activity in recordings as short as two seconds [4]. Identifying MUs from a short sequence is an advantage over other methods, such as spike-triggered averaging [9], which requires longer recordings due to other simultaneously active MUs and the motion of non-muscular structures hiding large parts of the movement caused by the target MU. Therefore, the blind source separation approach provides advantages compared to the spike-triggered averaging approach, such as lower memory and storage requirements and potential for, e.g. real-time imaging [41] and dynamic contractions applications. For these applications, future studies must consider the lower bound in terms of the recording duration to identify MUs and improve the classification of components into MUs or non-MUs using robust features or training a classifier. For example, the Gaussian-like 2D distribution of velocities reported in this work for the most repeatable components and similar to what has been found in previous studies [1, 4, 6, 7], may be a feature for the classification of a component as a MU. Thus, having a classifier for MU/non-MU-associated components enables the UUS approach to be stand-alone from HDsEMG.

A *k*-means algorithm with five clusters was used to generate binary maps from the spatial maps (output from decomposition algorithm) suitable for comparing the output between epochs. Five clusters were selected based on empirical observations that provided a robust and automatic way of thresholding the spatial map (figure S2 in the supplementary materials). We found that the spatial maps have pixel background values of slightly negative, slightly positive, and zero. The territory of interest has a range of positive values, much higher than the background, with the maximum value around the peak with decreasing values to the border. If we consider an extreme case where all the background pixels are zero, and thus one cluster. Then the territory will be divided into the remaining four clusters. Since we only take the cluster with the highest centroid value (figure S2 in the supplementary materials), we will get a few pixels in the selected cluster, which will then be compared to the selected centroid of the other two-second windows. However, we can see that the range of diameters of the selected clusters (table 1) is feasible regarding the expected size of a MU territory [34], which indicates that our selection is reasonable. Nevertheless, this parameter could be optimised further to improve the spatial repeatability values and

possibly numbers. That being said, it will not change the interpretation of our results, i.e. spatially repeatable components from UUS are associated with MU activity in human isometric contractions.

The fundamental signal obtained with the UUS is related to the force generated by muscle fibres. It should be comparable to forces generated during an unfused tetanic contraction in isometric conditions. This implies that we detect the subtle oscillations and no single twitch-like shapes, as they will likely have a duration exceeding the average inter-spike interval. Therefore, the amplitude and time parameters of the twitch-like shapes should be sensitive to preceding inter-spike intervals [42, 43]. That being said, it is possible to decompose these subtle oscillations obtained by UUS into twitch-like shapes [15]. However, we used spike-triggered averaging to get an average twitch, with every twitch normalised with mean zero and standard deviation equal to 1. We expect a causal relationship between the depolarisations along the fibre and the displacement due to the electromechanical coupling. Although a spike-triggered averaged twitch is interesting per se, we use the peak-to-peak spike-triggered averaged amplitudes *to select* which of all the decomposed components are associated with a MU.

While the study shows that spatially repeatable components from UUS are associated with MU activity in human isometric contractions, there are limitations. The UUS-based method relies on HDsEMG as a reference, which is limited to superficial MUs and sensitive to a thick subcutaneous fat layer [24, 44]. Future studies may consider an invasive EMG reference, such as fine-wire or thin-film multi-electrodes, to overcome this limitation [45]. Also, no technique can provide the full MU population, even in an optimal case. Moreover, we assume that MU activities can be linearly summed together in the velocity field. However, recent findings have observed non-linear summations [46]. Nevertheless, it should only affect the estimated temporal signals and not the spatial location of the MU during stable isometric contractions.

In conclusion, this study investigated the association of intra-sequence repeatable components with individual MU activity. We found that (1) spatial repeatability can be used as a data reduction to select putative MU activity during stable isometric contractions, and (2) the UUS decomposition method can identify possible MU activity in two-second recordings equally well as in eight-second recordings. These findings provide a foundation for developing stand-alone methods to identify MU in UUS and represent a step towards real-time imaging of active MU territories.

Data availability statement

The data cannot be made publicly available upon publication because no suitable repository exists for hosting data in this field of study. The data that support the findings of this study are available upon reasonable request from the authors.

Acknowledgments

R R is supported by the Swedish Research Council for Sport Science (Grant Number: D2023-0003). M C is supported by the project 'Trajector-AGE' (Grant Number: 2020477RW5PRIN), funded by the Italian Ministry of Universities and Research. C G is supported by the Swedish Research Council (Grant Number: 2022-04747).

ORCID iDs

Robin Rohlén https://orcid.org/0000-0003-4328-5467
Marco Carbonaro https://orcid.org/0000-0002-0877-7960
Giacinto L Cerone https://orcid.org/0000-0002-5295-5314
Kristen M Meiburger https://orcid.org/0000-0002-7302-6135
Alberto Botter https://orcid.org/0000-0002-4797-0667
Christer Grönlund https://orcid.org/0000-0003-4288-1208

References

[1] Deffieux T, Gennisson J L, Tanter M and Fink M 2008 Assessment of the mechanical properties of the musculoskeletal system using 2D and 3D very high frame rate ultrasound *IEEE Trans. Ultrason. Ferroelectr. Freq. Control* vol 55 pp 2177–90
[2] Grönlund C, Claesson K and Holtermann A 2013 Imaging two-dimensional mechanical waves of skeletal muscle contraction *Ultrasound Med. Biol.* **39** 360–9
[3] Rohlén R, Stålberg E, Stöverud K H, Yu J and Grönlund C 2020 A method for identification of mechanical response of motor units in skeletal muscle voluntary contractions using ultrafast ultrasound imaging—simulations and experimental tests *IEEE Access* **8** 50299–311
[4] Rohlén R, Stålberg E and Grönlund C 2020 Identification of single motor units in skeletal muscle under low force isometric voluntary contractions using ultrafast ultrasound *Sci. Rep.* **10** 1–11
[5] Ali H, Umander J, Rohlén R and Grönlund C 2020 A deep learning pipeline for identification of motor units in musculoskeletal ultrasound *IEEE Access* **8** 170595–608
[6] Carbonaro M, Meiburger K M, Seoni S, Hodson-Tole E F, Vieira T and Botter A 2022 Physical and electrophysiological motor unit characteristics are revealed with simultaneous high-density electromyography and ultrafast ultrasound imaging *Sci. Rep.* **12** 1–14
[7] Lubel E, Grandi-Sgambato B, Barsakcioglu D Y, Ibanez J, Tang M-X and Farina D 2022 Kinematics of individual muscle units in natural contractions measured *in vivo* using ultrafast ultrasound *J. Neural Eng.* **19** 056005
[8] Rohlén R, Yu J and Grönlund C 2022 Comparison of decomposition algorithms for identification of single motor units in ultrafast ultrasound image sequences of low force voluntary skeletal muscle contractions *BMC Res. Notes* **15** 207

[9] Carbonaro M, Zaccardi S, Seoni S, Meiburger K M and Botter A 2022 Detecting anatomical characteristics of single motor units by combining high density electromyography and ultrafast ultrasound: a simulation study *2022 44th Annual Int. Conf. IEEE Engineering in Medicine & Biology Society (EMBC)* (IEEE) pp 748–51

[10] Adrian E D and Bronk D W 1929 The discharge of impulses in motor nerve fibres: part II. The frequency of discharge in reflex and voluntary contractions *J. Physiol.* **67** 9–151

[11] Stålberg E and Antoni L 1980 Electrophysiological cross section of the motor unit *J. Neurol. Neurosurg. Psychiatry* **43** 469–74

[12] Daube J R and Rubin D I 2009 Needle electromyography *Muscle Nerve* **39** 244–70

[13] Fuglevand A J, Winter D A, Patla A E and Stashuk D 1992 Detection of motor unit action potentials with surface electrodes: influence of electrode size and spacing *Biol. Cybern.* **67** 143–53

[14] Farina D, Merletti R and Enoka R M 2014 The extraction of neural strategies from the surface EMG: an update *J. Appl. Physiol.* **117** 1215–30

[15] Rohlén R, Raikova R, Stålberg E and Grönlund C 2022 Estimation of contractile parameters of successive twitches in unfused tetanic contractions of single motor units—a proof-of-concept study using ultrafast ultrasound imaging *in vivo J. Electromyogr. Kinesiol.* **67** 102705

[16] Whittaker R G, Porcari P, Braz L, Williams T L, Schofield I S and Blamire A M 2019 Functional magnetic resonance imaging of human motor unit fasciculation in amyotrophic lateral sclerosis *Ann. Neurol.* **85** 455–9

[17] Birkbeck M G, Blamire A M, Whittaker R G, Sayer A A and Dodds R M 2020 The role of novel motor unit magnetic resonance imaging to investigate motor unit activity in ageing skeletal muscle *J. Cachexia Sarcopenia Muscle* **12** 17–29

[18] Waasdorp R, Mugge W, Vos H J, de Groot J H, Verweij M D, de Jong N, Schouten A C and Daeichin V 2021 Combining ultrafast ultrasound and high-density EMG to assess local electromechanical muscle dynamics: a feasibility study *IEEE Access* **9** 45277–88

[19] Sierra González D and Castellini C 2013 A realistic implementation of ultrasound imaging as a human-machine interface for upper-limb amputees *Front. Neurorobot.* **7** 17

[20] Dhawan A S, Mukherjee B, Patwardhan S, Akhlaghi N, Diao G, Levay G, Holley R, Joiner W M, Harris-Love M and Sikdar S 2019 Proprioceptive sonomyographic control: a novel method for intuitive and proportional control of multiple degrees-of-freedom for individuals with upper extremity limb loss *Sci. Rep.* **9** 1–15

[21] Rohlén R, Antfolk C and Grönlund C 2022 Optimization and comparison of two methods for spike train estimation in an unfused tetanic contraction of low threshold motor units *J. Electromyogr. Kinesiol.* **67** 102714

[22] Loupas T, Powers J T and Gill R W 1995 An axial velocity estimator for ultrasound blood flow imaging, based on a full evaluation of the Doppler equation by means of a two-dimensional autocorrelation approach *IEEE Trans. Ultrason. Ferroelectr. Freq. Control* **42** 672–88

[23] Holobar A and Zazula D 2007 Multichannel blind source separation using convolution kernel compensation *IEEE Trans. Signal Process.* **55** 4487–96

[24] Lulic-Kuryllo T and Inglis J G 2022 Sex differences in motor unit behaviour: a review *J. Electromyogr. Kinesiol.* **66** 102689

[25] Cerone G L, Giangrande A, Ghislieri M, Gazzoni M, Piitulainen H and Botter A 2022 Design and validation of a wireless body sensor network for integrated EEG and HD-sEMG acquisitions *IEEE Trans. Neural Syst. Rehabil. Eng.* **30** 61–71

[26] Cerone G L, Botter A and Gazzoni M 2019 A modular, smart, and wearable system for high density sEMG detection *IEEE Trans. Biomed. Eng.* **66** 3371–80

[27] Botter A, Vieira T M M, Loram I D, Merletti R and Hodson-Tole E F 2013 A novel system of electrodes transparent to ultrasound for simultaneous detection of myoelectric activity and B-mode ultrasound images of skeletal muscles *J. Appl. Physiol.* **115** 1203–14

[28] Børstad T K 2013 DSPView *MATLAB Central File Exchange*

[29] del Vecchio A, Holobar A, Falla D, Felici F, Enoka R M and Farina D 2020 Tutorial: analysis of motor unit discharge characteristics from high-density surface EMG signals *J. Electromyogr. Kinesiol.* **53** 102426

[30] Gallina A and Vieira T 2015 Territory and fiber orientation of vastus medialis motor units: a surface electromyography investigation *Muscle Nerve* **52** 1057–65

[31] Stone J V, Porrill J, Porter N R and Wilkinson I D 2002 Spatiotemporal independent component analysis of event-related fMRI data using skewed probability density functions *NeuroImage* **15** 407–21

[32] Farina D, Fattorini L, Felici F and Filligoi G 2002 Nonlinear surface EMG analysis to detect changes of motor unit conduction velocity and synchronization *J. Appl. Physiol.* **93** 1753–63

[33] Holobar A, Minetto M A and Farina D 2014 Accurate identification of motor unit discharge patterns from high-density surface EMG and validation with a novel signal-based performance metric *J. Neural Eng.* **11** 016008

[34] Stålberg E and Dioszeghy P 1991 Scanning EMG in normal muscle and in neuromuscular disorders *Electroencephalogr. Clin. Neurophysiol. Evoked Potentials* **81** 403–16

[35] Botter A, Vieira T, Carbonaro M, Cerone G L and Hodson-Tole E F 2021 Electrodes' configuration influences the agreement between surface EMG and B-mode ultrasound detection of motor unit fasciculation *IEEE Access* **9** 98110–20

[36] Hyvärinen A, Karhunen J and Oja E 2001 *Independent Component Analysis* (Wiley-Interscience)

[37] Wakeling J M, Ross S A, Ryan D S, Bolsterlee B, Konno R, Domínguez S and Nigam N 2020 The energy of muscle contraction. I. Tissue force and deformation during fixed-end contractions *Front. Physiol.* **11**

[38] Herzog W 2017 Skeletal muscle mechanics: questions, problems and possible solutions *J. NeuroEng. Rehabil.* **14** 98

[39] Kaczmarek P, Celichowski J, Drzymała-Celichowska H and Kasiński A 2009 The image of motor units architecture in the mechanomyographic signal during the single motor unit contraction: *in vivo* and simulation study *J. Electromyogr. Kinesiol.* **19** 553–63

[40] Negro F and Orizio C 2017 Robust estimation of average twitch contraction forces of populations of motor units in humans *J. Electromyogr. Kinesiol.* **37** 132–40

[41] Rohlén R, Lundsberg J, Malesevic N and Antfolk C A fast blind source separation algorithm for decomposing ultrafast ultrasound images into spatiotemporal muscle unit kinematics 2023 *J. Neural Eng.* **20** 034001

[42] Calancie B and Bawa P 1986 Limitations of the spike-triggered averaging technique *Muscle Nerve* **9** 78–83

[43] Nordstrom M A, Miles T S and Veale J L 1989 Effect of motor unit firing pattern on twitches obtained by spike-triggered averaging *Muscle Nerve* **12** 556–67

[44] Minetto M A, Botter A, Šprager S, Agosti F, Patrizi A, Lanfranco F and Sartorio A 2013 Feasibility study of detecting surface electromyograms in severely obese patients *J. Electromyogr. Kinesiol.* **23** 285–95

[45] Muceli S, Poppendieck W, Holobar A, Gandevia S, Liebetanz D and Farina D 2022 Blind identification of the spinal cord output in humans with high-density electrode arrays implanted in muscles *Sci. Adv.* **8** eabo5040

[46] Lubel E, Sgambato B G, Rohlén R, Ibáñez J, Barsakcioglu D Y, Tang M-X and Farina D 2023 Non-linearity in motor unit velocity twitch dynamics: implications for ultrafast ultrasound source separation (https://doi.org/10.1101/2023.03.24.533983)